IOP Publishing Rep. Prog. Phys. 89 (2026) 087501 https://doi.org/10.1088/1361-6633/ae8eaa

Reports on Progress in Physics

Check for updates

PAPER

The paradox of steady-state light diffusion

OPEN ACCESS

RECEIVED
14 April 2026

REVISED
7 July 2026

ACCEPTED FOR PUBLICATION
22 July 2026

PUBLISHED
11 August 2026

Original content from this work may be used under the terms of the Creative Commons Attribution 4.0 licence.

Any further distribution of this work must maintain attribution to the author(s) and the title of the work, journal citation and DOI.

André Liemert[1,†,*], **Lorenzo Pattelli**[2,3,†], **Alwin Kienle**[1], **Federico Tommasi**[4] and **Fabrizio Martelli**[4,*]

[1] Institut für Lasertechnologien in der Medizin und Meßtechnik an der Universität Ulm (ILM), Ulm, Germany
[2] Istituto Nazionale di Ricerca Metrologica (INRiM), Turin, Italy
[3] European Laboratory for Non-linear Spectroscopy (LENS), Sesto Fiorentino, Italy
[4] Dipartimento di Fisica e Astronomia, Università degli Studi di Firenze, Sesto Fiorentino, Italy
[†] These authors contributed equally to this work.
[*] Authors to whom any correspondence should be addressed.

E-mail: andre.liemert@ilm-ulm.de and fabrizio.martelli@unifi.it

Keywords: diffusion theory, radiative transfer theory, diffusion coefficient, absorption coefficient, scattering anisotropy, diffusion equation, radiative transfer equation

Corresponding editor: Dr Paul Mabey

Abstract

For over thirty years, the definition of the diffusion coefficient in light transport has been the subject of persistent debate. Its canonical expression includes an explicit dependence on absorption, violating a fundamental scaling property of the radiative transfer equation (RTE). In the time domain (TD), evidence shows that the correct definition is independent of absorption, yet absorption-dependent formulations unfortunately remain common in practical data analysis. In the continuous-wave regime, the radial decay of the RTE can be reproduced by an absorption-dependent coefficient, but this does not imply that steady-state transport is genuinely diffusive. Here, this controversy is resolved through an exact consistency test based solely on the requirement that diffusion converges to the RTE in the limit of infinite propagation. In the TD, we prove that the absorption-independent coefficient is both necessary and sufficient for exact long-time convergence. In the continuous-wave regime, we prove analytically that no scalar diffusion coefficient can make diffusion asymptotically equivalent to the RTE when absorption is nonzero: matching the dominant attenuation length fixes one coefficient, whereas matching the residue requires a different one. We further show that this failure is not caused by any finite set of ballistic or few-scattering contributions, and quantify the intrinsic error introduced by incorrect parameterizations in idealized absorption-retrieval scenarios. These results establish the time-domain formulation as the only self-consistent reference and call for a re-examination of how diffusion is applied in optical transport studies

1. Introduction

The diffusion equation (DE) is a cornerstone of transport theory, as it provides a robust and closed-form approximation of the more exact but less tractable radiative transfer equation (RTE). The validity of this approximation relies on the physical expectation that a classical radiative transfer process becomes diffusive in the limit of infinite scattering events. For this reason, it is widely agreed that the DE should become increasingly accurate in the long-time and large-distance asymptotic limits when pulsed and steady-state sources are considered, respectively. On other aspects, however, general consensus is lacking. One particularly persistent and consequential controversy concerns the correct expression of the diffusion coefficient D appearing in the DE—a debate that has remained unresolved for more than thirty years. The controversy originates from the fact that, when the DE is derived from the RTE, a diffusion coefficient that depends on the absorption coefficient μ_a is obtained as [1]

$$D = \left[3\left(\mu_s' + \mu_a\right)\right]^{-1}, \tag{1}$$

© 2026 The Author(s). Published by IOP Publishing Ltd

where μ_s' is the reduced scattering coefficient of the medium.

This result has long been considered problematic by part of the scientific community, as it violates the fundamental scaling law of radiative transfer with respect to absorption because the Beer–Lambert–Bouguer absorption scaling is not preserved when D is made to depend on μ_a through (1) [2–6]. For years, a seemingly ad hoc but physically motivated solution to enforce the correct scaling consisted of deriving D in the absorption-less case

$$D = (3\mu_s')^{-1}, \tag{2}$$

and then including absorption separately as an attenuation factor to the time-domain solution according to the microscopic Beer–Lambert–Bouguer law [2, 7, 8]. This strategy was later revisited by Pierrat *et al* [9], who used a singular eigenfunction expansion approach to the RTE to support the validity of the absorption-independent definition of the diffusion coefficient in the time domain (TD).

However, this insight has not led to a consensus, which can be at least partly ascribed to the fact that most studies suffer from instrumental limitations or rely on Monte Carlo simulations for validation, which are inherently noisy and unable to resolve small asymptotic discrepancies—especially when absorption is low, as is typically required for the diffusion approximation to hold.

This situation has led to a highly fragmented literature, where different models and conventions coexist with little cross-validation. The ambiguity is not merely historical: it is still reported in recent reviews of time-domain diffuse optics [10], while the absorption-dependent expression continues to appear in practical TD applications. Typical examples include biomedical or *in vivo* time-domain experiments, where distributions of the time-of-flight or time-resolved reflectance curves are fitted using $D = 1/[3(\mu_a + \mu_s')]$ [11–14]. Similar uses occur in time-of-flight imaging, scattering-media reconstruction, and transport-information studies [15–19], as well as in numerical, material, or model-development contexts [20–23]. Adding to this complexity, the original problematic expression (1) has evolved into a family of parametrized expressions with tuneable absorption dependence [3, 6, 24–29], usually written in the form:

$$D = [3(\mu_s' + a\mu_a)]^{-1}, \tag{3}$$

with a as an adjustable parameter. Suggested values include $a = 1$ [8, 27], $a = 1/3$ [26] or $a = 1/5$ [3], as well as a range of other values [6, 24, 25, 28, 30–32], motivated by attempts to improve agreement between the DE and the RTE at short times, or close to boundaries, or for low albedo conditions. Especially in these regimes, the DE is expected to become less accurate so that introducing such modifications can improve agreement at finite times or distances. However, assigning a physical meaning to these corrections remains questionable and comes at the cost of ultimately breaking the correct scaling of the DE in the TD, introducing systematic biases in the analysis of experimental and numerical data.

To date, several attempts have been made to resolve this ambiguity focusing on both the continuous-wave and time-domain regimes, for instance by resorting to the telegrapher equation as a simpler proxy to the RTE [26], or to a truncated cumulant approximation [6] or to heuristic versions of its solution [33]. However, all expressions akin to (3) eventually converge trivially to (2) in the limit of vanishing absorption, meaning that the discrepancies between different definitions of D also become vanishingly small and difficult to tell apart within the uncertainty of experimental measurements or the finite statistics of numerical simulations. For these reasons, a conclusive resolution of this issue can only be reached via an analytical argument.

In this work, we provide an exact and physically intuitive analysis of this problem by taking the asymptotic convergence to the RTE as the defining requirement for a diffusion coefficient. To this purpose, we start from exact solutions of the RTE in an infinite homogeneous medium with general anisotropic scattering [34–37], and derive the asymptotic form of the fluence for both the TD (section 2) and continuous wave (CW) regimes (section 3). In the TD regime, this criterion gives a genuine equivalence: equation (2) is both necessary and sufficient for asymptotic convergence, irrespective of scattering anisotropy. In the CW regime, the same test exposes a stronger failure. For isotropic scattering we prove analytically that the coefficient required to match the dominant RTE attenuation length differs from the coefficient required to reproduce the leading residue; for anisotropic scattering, the same incompatibility is identified from the dominant P_N mode. We also show that removing ballistic and any fixed finite number of low-scattering contributions does not change the CW asymptotic pole or residue, and we quantify the scale of the resulting absorption-retrieval bias in an idealized fitting scenario. Implications of these findings, also with respect to the previous literature on this topic, are discussed in section 4, showing that only a time-domain description of diffusion is consistent with its premises, and should therefore be taken as the reference. Finally, practical conclusions are drawn in section 5.

2. Infinite time-asymptotic limit

The aim of this section is to study the time-asymptotic limit of the RTE in the TD. To do so, we consider its analytical solution for the paradigmatic case of an infinite medium [35, 36], compute its limit for $t \to \infty$ for both the isotropic and anisotropic case, and show that this limit coincides with the well-known solution of the DE *if and only if* an absorption-independent diffusion coefficient is used. Mathematically, this can be stated as

$$\lim_{t\to\infty} \frac{\phi(r,t)}{\psi(r,t)} = 1 \iff D = \frac{1}{3}\frac{1}{\mu_s'}, \tag{4}$$

where $\mu_s = \mu_s'$ in the case of isotropic scattering. Here and in the following, Φ will be used to denote the exact RTE fluence, ϕ represents its dominant asymptotic term, and ψ denotes the corresponding DE candidate. This notation is used consistently throughout the paper for both isotropic and anisotropic scattering.

2.1. Isotropic scattering

In the case of isotropic scattering, the exact fluence admits a convenient integral representation and the asymptotic ratio between ϕ and ψ can be evaluated explicitly. The starting point to calculate both terms is the exact fluence $\Phi(r,t) = 2\pi \int_{-1}^{1} I(r,\cos\theta,t)\,\mathrm{d}\cos\theta$ obtained from the radiance $I = I(r,\cos\theta,t)$ which satisfies the time dependent RTE [8]. For isotropic scattering, we then have

$$\frac{1}{c}\frac{\partial I}{\partial t} + \cos\theta\frac{\partial I}{\partial r} + \frac{1-\cos^2\theta}{r}\frac{\partial I}{\partial \cos\theta} + (\mu_s+\mu_a)I = \frac{\mu_s}{4\pi}\Phi, \tag{5}$$

where $I(r,\cos\theta,0) = c\delta(r)(4\pi r)^{-2}$ is the corresponding initial condition, μ_s is the scattering coefficient, c is the speed of light, and $\cos\theta$ identifies the direction along which I is evaluated. This equation can be solved in different ways, e.g. by using a combined Fourier-Laplace transform method. In terms of the fluence, this method yields the following expression [35]:

$$\begin{aligned}\Phi(r,t) = \Phi_0(r,t) + \Phi_1(r,t) + \frac{\mu_s{}^2 \mathrm{e}^{-(\mu_s+\mu_a)ct}}{16\pi^2 rt}\int_0^r \left|\frac{ct-\eta}{ct+\eta}\right|^{\mu_s\frac{r-\eta}{2}} \left[\left(\pi^3 - 3\pi\ln^2\frac{ct-\eta}{ct+\eta}\right)\cos\left(\pi\mu_s\frac{r-\eta}{2}\right)\right.\\ \left. + \ln\frac{ct-\eta}{ct+\eta}\left(3\pi^2 - \ln^2\frac{ct-\eta}{ct+\eta}\right)\sin\left(\pi\mu_s\frac{r-\eta}{2}\right)\right]\mathrm{d}\eta + \frac{\mathrm{e}^{-\mu_a ct}}{2\pi^2 r}\int_0^{\pi\mu_s/2}\hat{u}(k,t)\sin(kr)\,k\,\mathrm{d}k,\end{aligned} \tag{6}$$

for $ct > r$ due to the finite speed of propagation. The function $\hat{u}$ in Fourier space is given by [35]

$$\hat{u}(k,t) := c\frac{\mathrm{e}^{[k\cot(k/\mu_s)-\mu_s]ct}}{\mathrm{sinc}^2(k/\mu_s)}, \tag{7}$$

for $(k,t) \in [0,\pi\mu_s/2] \times \mathbb{R}_0^+$, and $\mathrm{sinc}\,x := \frac{1}{x}\sin x$. Furthermore, the ballistic and single-scattering fluence contributions are defined as

$$\Phi_0(r,t) = c\frac{\delta(r-ct)}{4\pi r^2}\mathrm{e}^{-(\mu_s+\mu_a)ct}, \tag{8}$$

$$\Phi_1(r,t) = \frac{\mu_s}{4\pi rt}\mathrm{e}^{-(\mu_s+\mu_a)ct}\ln\frac{ct+r}{ct-r}. \tag{9}$$

The first integral in (6) vanishes exponentially. To see this, we note that

$$\begin{aligned}\left|\int_0^r(\cdot)\,\mathrm{d}\eta\right| &\leqslant \int_0^r\left[\left|\pi^3 - 3\pi\ln^2\frac{ct-\eta}{ct+\eta}\right| + \ln\frac{ct+\eta}{ct-\eta}\left|3\pi^2 - \ln^2\frac{ct-\eta}{ct+\eta}\right|\right]\mathrm{d}\eta\\ &\leqslant r\left[\pi + 2\,\mathrm{artanh}\left(\frac{r}{ct_0}\right)\right]^3 \quad \text{for all } t > t_0 > r/c,\end{aligned}$$

where we have used $|(ct-\eta)/(ct+\eta)| \leqslant 1$ for $\eta \in [0,r]$ and $|\ln x| = |\ln\frac{1}{x}|$. This upper bound is additionally damped by the factor $\mathrm{e}^{-(\mu_s+\mu_a)ct}$ so that it exhibits (like the ballistic and the single-scattered fluence) an exponential decay at late times. As shown below, the leading term in the long-time limit will be extracted from the last integral in (6). In view of (4), we start by demonstrating the '$\Longleftarrow$' side of the implication. We begin with identifying an approximate expression for the asymptotic fluence ψ, i.e. a function that represents the infinite-time asymptotic limit of Φ, via plausibility assessments. Let us consider the last term in (6) that is given by

$$u(r,t) = \frac{1}{2\pi^2 r}\int_0^{\pi\mu_s/2} \hat{u}(k,t)\sin(kr)\,k\,\mathrm{d}k,$$

and note that $\hat{u}(k,t)$ tends rapidly to zero (for every $k>0$) for large times due to the exponential in (7). We therefore focus on the behavior of $\hat{u}$ near $k=0$ under the use of the Taylor expansions

$$k\cot(k/\mu_s) - \mu_s = -\frac{k^2}{3\mu_s} - \frac{k^4}{45{\mu_s}^3} + \mathcal{O}\left(k^6\right), \quad |k| < \pi\mu_s,$$

$$\operatorname{sinc}\left(\frac{k}{\mu_s}\right) = 1 - \frac{1}{3!}\frac{k^2}{{\mu_s}^2} + \frac{1}{5!}\frac{k^4}{{\mu_s}^4} + \mathcal{O}\left(k^6\right), \quad k \in \mathbb{R},$$

where the condition $|k| < \pi\mu_s$ is automatically satisfied due to the upper limit of integration. Next, inspired by the leading term in the cotangent series for small spatial frequencies k, we identify the diffusion coefficient $D := 1/(3\mu_s)$ (having no absorption) and remark that $\hat{u}(k,t) \approx c\mathrm{e}^{-Dck^2t}$ as $k \to 0$ (i.e. the first term dominates over the others). Additionally, as is frequently done in the asymptotic analysis of integrals, we extend the upper limit of integration to infinity, exploiting the fact that the exponential term decays so quickly that the integral can be run to infinity without affecting the final result. This yields the following candidate for the asymptotic fluence:

$$\psi(r,t) := \frac{c\mathrm{e}^{-\mu_a ct}}{2\pi^2 r}\int_0^\infty \mathrm{e}^{-Dck^2t}\sin(kr)\,k\,\mathrm{d}k, \tag{10}$$

which should be an adequate approximation in the long-time limit. This integral can be evaluated analytically [38], yielding

$$\psi(r,t) = \frac{c\mathrm{e}^{-\mu_a ct}}{(4\pi Dct)^{3/2}}\mathrm{e}^{-r^2/(4Dct)}, \tag{11}$$

which coincides with the well-known DE solution for the fluence, with D independent of absorption. This approximation reflects the exact RTE scaling with absorption, as μ_a appears only in the exponential term, in accordance with the Beer–Lambert–Bouguer law.

In the following, we prove that the diffusion-like solution (11), which has been derived via plausibility assessments, agrees exactly with the transport theory fluence from (6) as $t \to \infty$. This, in turn, will show that $D = 1/(3\mu_s) \implies \lim_{t\to\infty}\phi(r,t)/\psi(r,t) = 1$. For this purpose, we proceed by splitting the integral representation for u into two parts, namely

$$u(r,t) = \frac{1}{2\pi^2 r}\left[\int_0^{\varepsilon(t)} (\cdot)\,\mathrm{d}k + \int_{\varepsilon(t)}^{\pi\mu_s/2} (\cdot)\,\mathrm{d}k\right], \tag{12}$$

with an integration limit $\varepsilon(t) \in (0, \pi\mu_s/2)$ that satisfies $\varepsilon(t) \to 0$ as $t \to \infty$. This integral converges numerically to the correct infinite-time asymptotic limit for any choice of $\varepsilon(t)$ in the target interval. However, the dominant term can also be isolated analytically by selecting a suitable decay rate for $\varepsilon(t)$ such as $\varepsilon(t) \sim t^{-1/\alpha}$ (for instance, $\varepsilon(t) = (D^2ct)^{-1/3}$, having the expected units of m^{-1}). The range of permissible values for α follows during the next derivation steps. We continue with the second integral of (12) that can be bounded according to

$$\left|\int_{\varepsilon(t)}^{\pi\mu_s/2} \hat{u}(k,t)\sin(kr)\,k\,\mathrm{d}k\right| \leqslant \frac{c\pi^2}{4}\int_{\varepsilon(t)}^\infty \mathrm{e}^{-Dctk^2}k\,\mathrm{d}k = \frac{\pi^2}{8Dt}\mathrm{e}^{-Dct\varepsilon^2(t)}, \tag{13}$$

where we have used $|\sin x| \leqslant 1$ for all $x \in \mathbb{R}$, $\operatorname{sinc} x \geqslant 2/\pi$ for $|x| \leqslant \pi/2$, and

$$\hat{u}(k,t) \leqslant c(\pi/2)^2\,\mathrm{e}^{-Dctk^2} \quad \text{on } [0, \pi\mu_s/2] \times \mathbb{R}_0^+.$$

The behavior of the exponential in (13) depends on the parameter α, due to $t\varepsilon^2(t) \sim t^{1-2/\alpha}$. Thus, in order to get for this term an exponential decay (which requires $\lim_{t\to\infty} t\varepsilon^2(t) \to \infty$), we have to ensure that $1 - 2/\alpha > 0$, yielding the lower bound $\alpha > 2$.

On the other hand, the first integral in (12) can be handled by the mean value theorem for integrals. For sufficiently large t, the cutoff satisfies $\varepsilon(t) < \pi/r$, so that $\sin(kr) \geqslant 0$ throughout the interval $0 \leqslant k \leqslant \varepsilon(t)$. The remaining factor multiplying $\sin(kr)k$ is continuous on this interval. Therefore, there exists a point $\xi = \xi(t) \in [0, \varepsilon(t)]$ such that

$$\int_0^{\varepsilon(t)} \mathrm{e}^{-Dck^2t} \frac{\mathrm{e}^{\vartheta(k)ct}}{\operatorname{sinc}^2(k/\mu_\mathrm{s})} \sin(kr)\, k\, \mathrm{d}k = \frac{\mathrm{e}^{\vartheta(\xi)ct}}{\operatorname{sinc}^2(\xi/\mu_\mathrm{s})} \int_0^{\varepsilon(t)} \mathrm{e}^{-Dck^2t} \sin(kr)\, k\, \mathrm{d}k. \tag{14}$$

The monotonically decreasing function $\vartheta \leqslant 0$ is defined as

$$\vartheta(k) := k\cot(k/\mu_\mathrm{s}) - \mu_\mathrm{s} + Dk^2 = -\frac{k^4}{45\mu_\mathrm{s}^3} + \mathcal{O}(k^6), \quad 0 \leqslant k \leqslant \pi\mu_\mathrm{s}/2.$$

It remains to show that

$$\lim_{t\to\infty} \frac{\mathrm{e}^{\vartheta(\xi)ct}}{\operatorname{sinc}^2(\xi/\mu_\mathrm{s})} = 1 \quad \text{for all}\, \xi = \xi(t). \tag{15}$$

Since $0 \leqslant \xi(t) \leqslant \varepsilon(t)$ and $\lim_{t\to\infty}\varepsilon(t) = 0$, the sandwich theorem gives $\lim_{t\to\infty}\xi(t) = 0$. This, in turn, implies $\lim_{t\to\infty}\operatorname{sinc}^2(\xi/\mu_\mathrm{s}) = 1$. Moreover, since $\vartheta(k) = -k^4/(45\mu_\mathrm{s}^3) + \mathcal{O}(k^6)$ near the origin, there are constants $C > 0$ and $k_0 > 0$ such that $-Ck^4 \leqslant \vartheta(k) \leqslant 0$ for $0 \leqslant k \leqslant k_0$. For sufficiently large t, $\varepsilon(t) < k_0$ and the monotonicity of ϑ gives

$$0 \leqslant \xi(t) \leqslant \varepsilon(t) \quad \Longrightarrow \quad 1 \geqslant \mathrm{e}^{\vartheta(\xi)ct} \geqslant \mathrm{e}^{-cCt\varepsilon^4(t)}.$$

Thus, $t\varepsilon^4(t) \to 0$ is sufficient to obtain $\mathrm{e}^{\vartheta(\xi)ct} \to 1$ uniformly for every admissible intermediate point $\xi(t)$, and hence to prove (15). For $\varepsilon(t) \sim t^{-1/\alpha}$ this condition gives $1 - 4/\alpha < 0$, i.e. $\alpha < 4$. Together with the lower bound $\alpha > 2$ obtained from the complementary integral, this yields the admissible range $2 < \alpha < 4$. The same estimate also shows that the prefactor in (14) differs from unity by at most $\mathcal{O}(t^{1-4/\alpha})$. At this point, u from (12) can be represented in the form

$$u(r,t) = \frac{c}{2\pi^2 r} \frac{\mathrm{e}^{\vartheta(\xi)ct}}{\operatorname{sinc}^2(\xi/\mu_\mathrm{s})} \int_0^{\varepsilon(t)} \mathrm{e}^{-Dctk^2} \sin(kr)\, k\, \mathrm{d}k + \mathcal{O}\left(t^{-1}\mathrm{e}^{-Dct\varepsilon^2(t)}\right), \tag{16}$$

as $t \to \infty$. For evaluation of the remaining integral, we make use of

$$\int_0^{\varepsilon(t)} \mathrm{e}^{-Dctk^2} \cos(kr)\, \mathrm{d}k = \sqrt{\frac{\pi}{4Dct}} \mathrm{e}^{-r^2/(4Dct)} \mathrm{Re}\{\mathrm{erf}\left(\varepsilon(t)\sqrt{Dct} - \mathrm{i}r/\sqrt{4Dct}\right)\},$$

in combination with the relation $k\sin(kr) = -\frac{\mathrm{d}}{\mathrm{d}r}\cos(kr)$. Here, $\mathrm{erf}\, z = (2/\sqrt{\pi})\int_0^z \mathrm{e}^{-t^2}\,\mathrm{d}t$ denotes the error function [38]. Thus, after the integration has been carried out, we have to calculate the negative derivative with respect to r. We then obtain for u from (16) the time evolution

$$\begin{aligned} u(r,t) = \frac{\mathrm{e}^{\vartheta(\xi)ct}}{\operatorname{sinc}^2(\xi/\mu_\mathrm{s})} &\left[\frac{c}{(4\pi Dct)^{3/2}} \mathrm{e}^{-r^2/(4Dct)}\, \mathrm{Re}\left\{\mathrm{erf}\left(\varepsilon(t)\sqrt{Dct} - \mathrm{i}r/\sqrt{4Dct}\right)\right\}\right. \\ &\left. -\frac{1}{4\pi^2 Dtr} \sin(\varepsilon(t)r)\, \mathrm{e}^{-Dct\varepsilon^2(t)}\right] + \mathcal{O}\left(t^{-1}\mathrm{e}^{-Dct\varepsilon^2(t)}\right). \end{aligned}$$

Using this and setting $\phi(r,t) = \mathrm{e}^{-\mu_\mathrm{a}ct}u(r,t)$, we can form the ratio

$$\begin{aligned} \frac{\phi(r,t)}{\psi(r,t)} = \frac{\mathrm{e}^{\vartheta(\xi)ct}}{\operatorname{sinc}^2(\xi/\mu_\mathrm{s})} &\left[\mathrm{Re}\left\{\mathrm{erf}\left(\varepsilon(t)\sqrt{Dct} - \mathrm{i}r/\sqrt{4Dct}\right)\right\}\right. \\ &\left. -\sqrt{\frac{4Dct}{\pi}} \frac{\sin(\varepsilon(t)r)}{r} \mathrm{e}^{-Dct\varepsilon(t)^2 + r^2/(4Dct)}\right] + \mathcal{O}\left(\sqrt{t}\mathrm{e}^{-Dct\varepsilon^2(t)}\right). \end{aligned} \tag{17}$$

Recalling (15), together with $\varepsilon(t)\sqrt{Dct} \to \infty$ and $r/\sqrt{4Dct} \to 0$, the error-function term tends to unity and we directly obtain the limit: $\lim_{t\to\infty}\phi(r,t)/\psi(r,t) = 1$. This completes the first part of the proof, i.e. $D = 1/(3\mu_\mathrm{s}) \implies \lim_{t\to\infty}\phi(r,t)/\psi(r,t) = 1$. We emphasize once again that the diffusion coefficient emerges in this procedure naturally (without absorption), because it derives directly from the series expansion of the cotangent of the exact fluence obtained from transport theory. This differs from the classical derivation of the DE, in which higher order time derivatives are intentionally discarded at the beginning of the derivation, leading to the appearance of a spurious absorption term in the diffusion coefficient.

Proving the reverse implication in (4), i.e. $\lim_{t\to\infty}\phi(r,t)/\psi(r,t)=1 \implies D=1/(3\mu_\mathrm{s})$, is simpler, as it can be performed via contraposition. Let us assume an arbitrary diffusion coefficient $\kappa\neq D$ and denote its corresponding asymptotic expression by $\tilde{\psi}$ (in contrast to ψ from (11), where D does not depend on absorption). Then, instead of (17), we obtain the following modified ratio

$$\frac{\phi(r,t)}{\tilde{\psi}(r,t)}=\frac{\mathrm{e}^{\vartheta(\xi)ct}}{\mathrm{sinc}^2(\xi/\mu_\mathrm{s})}\left[\left(\frac{\kappa}{D}\right)^{3/2}\mathrm{Re}\left\{\mathrm{erf}\left(\varepsilon(t)\sqrt{Dct}-\mathrm{i}r/\sqrt{4Dct}\right)\right\}\mathrm{e}^{\frac{r^2}{4ct}\left(\frac{1}{\kappa}-\frac{1}{D}\right)}\right.$$
$$\left.-\sqrt{\frac{4\kappa ct}{\pi}}\frac{\sin(\varepsilon(t)r)}{r}\frac{\kappa}{D}\mathrm{e}^{-Dct\varepsilon(t)^2+r^2/(4\kappa ct)}\right]+\mathcal{O}\left(\sqrt{t}\mathrm{e}^{-Dct\varepsilon^2(t)}\right),$$

with $\lim_{t\to\infty}\phi(r,t)/\tilde{\psi}(r,t)=(\kappa/D)^{3/2}\neq 1$. In particular, for the parametrization proposed in literature, $\kappa=1/[3(a\mu_\mathrm{a}+\mu_\mathrm{s})]$, we get

$$\lim_{t\to\infty}\frac{\phi(r,t)}{\tilde{\psi}(r,t)}=\left(\frac{\mu_\mathrm{s}}{a\mu_\mathrm{a}+\mu_\mathrm{s}}\right)^{3/2}<1\quad\text{for all}\,a>0.$$

This confirms our initial assertion (4).

2.2. Anisotropic scattering

The aim of this section is to complete the analysis of the asymptotic time limit for the anisotropic scattering case. The procedure used is different from the previous one since the representation of the solution cannot be given in the same form available for isotropic scattering. In fact, the time-dependent fluence for an anisotropically scattering medium cannot be written in terms of a single quadrature such as (6). However, it can be evaluated by means of the matrix exponential method used to approach the time-dependent RTE [36]. The resulting RTE fluence in space-time domain becomes

$$\Phi(r,t)=\frac{c}{2\pi^2 r}\int_0^\infty \hat{\boldsymbol{e}}_0^T\mathrm{e}^{-Act}\hat{\boldsymbol{e}}_0\sin(kr)\,k\,\mathrm{d}k, \tag{18}$$

where $A\in\mathbb{C}^{(N+1)\times(N+1)}$ is explicitly given in [36], $\hat{\boldsymbol{e}}_0=(1,0,\ldots,0)^T\in\mathbb{R}^{N+1}$ and $N\geqslant 1$ is a sufficiently large odd number that corresponds to the P_N approximation order. This RTE solution provides a complete description of the time-domain anisotropic propagation in an infinite medium.

In the case of anisotropic scattering, although analytic solutions such as (18) exist, closed-form analytical solutions for the exact transport-theory fluence are not available either in real space or in Fourier space. Nevertheless, information on long-time behavior can also be extracted by means of spatial moments. In general, if the moments

$$R_\ell := \frac{4\pi}{2\ell+1}\int_0^\infty r^{2\ell}f(r)r^2\,\mathrm{d}r,\quad \ell\in\mathbb{N}_0,$$

exist and are known, an exact (local) representation of the spherically symmetric Fourier transform $\hat{f}(k)=(4\pi/k)\int_0^\infty f(r)\sin(kr)r\,\mathrm{d}r$ is available in the form of the Taylor series

$$\hat{f}(k)=\sum_{\ell=0}^\infty\frac{(-1)^\ell R_\ell}{(2\ell)!}k^{2\ell}=\sum_{\ell=0}^\infty\frac{\hat{f}^{(2\ell)}(0)}{(2\ell)!}k^{2\ell}. \tag{19}$$

To find the spatial moments for the fluence, we first consider the representation [36]

$$\hat{\Phi}(k,s)=\hat{\boldsymbol{e}}_0^T(\Sigma+\mathrm{i}kM)^{-1}\hat{\boldsymbol{e}}_0, \tag{20}$$

with $\hat{\Phi}$ being the Fourier-Laplace transform of (18) and the symmetric matrix M is defined as

$$M=\begin{pmatrix} 0 & \frac{1}{\sqrt{3}} & 0 & \cdots & 0\\ \frac{1}{\sqrt{3}} & 0 & \frac{2}{\sqrt{15}} & \cdots & 0\\ 0 & \frac{2}{\sqrt{15}} & 0 & \cdots & 0\\ \vdots & \vdots & \vdots & \ddots & \frac{N}{\sqrt{4N^2-1}}\\ 0 & 0 & 0 & \frac{N}{\sqrt{4N^2-1}} & 0\end{pmatrix}.$$

It is important to note (as explicitly shown below) that the limiting diffusion coefficient obtained below is independent of the chosen P_N order N. Due to the first shifting theorem for the Laplace transform [38], the absorption term can be dropped here and be reconsidered afterwards by multiplication with the factor $\mathrm{e}^{-\mu_a ct}$ (see appendix). The diagonal matrix $\Sigma \in \mathbb{C}^{(N+1)\times(N+1)}$ contains the information about the scattering phase function $f(\hat{\boldsymbol{s}},\hat{\boldsymbol{s}}') = f(\hat{\boldsymbol{s}}\cdot\hat{\boldsymbol{s}}')$ and it is given by [36]:

$$\Sigma = \Sigma(s) = \mathrm{diag}(\sigma_0, \sigma_1, \ldots, \sigma_N), \tag{21}$$

where $\sigma_\ell := \mu_s(1-f_\ell) + s/c$, s is the Laplace-transform variable, and f_ℓ are the Legendre moments of the scattering phase function, which are given by:

$$f(\cos\theta) = \sum_{\ell=0}^{\infty} \frac{2\ell+1}{4\pi} f_\ell P_\ell(\cos\theta), \quad \text{where} \quad f_\ell = 2\pi \int_{-1}^{1} f(\cos\theta) P_\ell(\cos\theta)\,\mathrm{d}\cos\theta.$$

In particular, we have $f_1 = g$ as the anisotropy factor. The determination of the spatial moments for the fluence requires the $2\ell^{\mathrm{th}}$ derivative of (20) at $k=0$, cf also (19). To find this, we introduce $\hat{\boldsymbol{\Phi}}(k,s) = (\Sigma + \mathrm{i}kM)^{-1}\hat{\boldsymbol{e}}_0$ and note that the fluence from (20) is the first component of $\hat{\boldsymbol{\Phi}}$, which means $\hat{\Phi} = \hat{\boldsymbol{e}}_0^T\hat{\boldsymbol{\Phi}}$. For this introduced vector-valued function, the $2\ell^{\mathrm{th}}$ derivative at $k=0$ can be evaluated directly. In doing so, we apply the operator $\frac{\mathrm{d}^{2\ell}}{\mathrm{d}k^{2\ell}}$ on both sides of the equation $(\Sigma + \mathrm{i}kM)\hat{\boldsymbol{\Phi}}(k,s) = \hat{\boldsymbol{e}}_0$, yielding

$$\mathbf{0} = \frac{\mathrm{d}^{2\ell}}{\mathrm{d}k^{2\ell}}\left[(\Sigma + \mathrm{i}kM)\hat{\boldsymbol{\Phi}}(k,s)\right] = (\Sigma + \mathrm{i}kM)\hat{\boldsymbol{\Phi}}^{(2\ell)}(k,s) + 2\mathrm{i}\ell M\hat{\boldsymbol{\Phi}}^{(2\ell-1)}(k,s).$$

Next, after setting $k=0$, we successively find

$$\begin{aligned}\hat{\boldsymbol{\Phi}}^{(2\ell)}(0,s) &= (-\mathrm{i})\,2\ell\left(\Sigma^{-1}M\right)\hat{\boldsymbol{\Phi}}^{(2\ell-1)}(0,s) = (-\mathrm{i})^2\,2\ell(2\ell-1)\left(\Sigma^{-1}M\right)^2\hat{\boldsymbol{\Phi}}^{(2\ell-2)}(0,s)\\ &= \cdots = (-\mathrm{i})^{2\ell}(2\ell)!\left(\Sigma^{-1}M\right)^{2\ell}\hat{\boldsymbol{\Phi}}^{(0)}(0,s) = (-1)^{\ell}(2\ell)!\left(\Sigma^{-1}M\right)^{2\ell}\hat{\boldsymbol{\Phi}}(0,s).\end{aligned}$$

From $\Sigma\hat{\boldsymbol{\Phi}}(0,s) = \hat{\boldsymbol{e}}_0$, we obtain $\hat{\boldsymbol{\Phi}}(0,s) = \Sigma^{-1}\hat{\boldsymbol{e}}_0 = (c/s)\hat{\boldsymbol{e}}_0$, and hence the moments turn out to be:

$$R_\ell(s) = (-\mathrm{i})^{2\ell}\hat{\Phi}^{(2\ell)}(0,s) = (-1)^{\ell}\hat{\boldsymbol{e}}_0^T\hat{\boldsymbol{\Phi}}^{(2\ell)}(0,s) = \frac{(2\ell)!}{s/c}\hat{\boldsymbol{e}}_0^T\left(\Sigma^{-1}M\right)^{2\ell}\hat{\boldsymbol{e}}_0, \quad \ell \in \mathbb{N}_0. \tag{22}$$

Considered as a function of s, the moments R_ℓ are rational functions. As mentioned above, the long-time diffusion coefficient obtained from these moments is independent of the parameter N. To verify this, let us first examine the following limit:

$$\lim_{s\to 0}(s/c)\left(\Sigma^{-1}M\right)^2 = \begin{bmatrix} D & 0 & \frac{2}{\sqrt{5}}D & 0 & \cdots \\ 0 & D & 0 & 0 & \cdots \\ 0 & 0 & 0 & 0 & \cdots \\ \vdots & \vdots & \vdots & \vdots & \ddots \end{bmatrix} \tag{23}$$

with $D := 1/(3\mu_s')$ and $\mu_s' := \mu_s(1\text{–}g)$, showing that only three entries remain non-zero (see appendix).

With this result, we find

$$\lim_{s\to 0}\hat{\boldsymbol{e}}_0^T(s/c)^{\ell}\left(\Sigma^{-1}M\right)^{2\ell}\hat{\boldsymbol{e}}_0 = \hat{\boldsymbol{e}}_0^T\left(\lim_{s\to 0}(s/c)\left(\Sigma^{-1}M\right)^2\right)^{\ell}\hat{\boldsymbol{e}}_0 = D^{\ell}.$$

This, in turn, by considering the moments of (22), gives

$$\lim_{s\to 0}(s/c)^{\ell+1}R_\ell(s) = (2\ell)!D^{\ell},$$

showing that R_ℓ has at $s=0$ a pole of the maximal order $\ell+1$. We note that there are no poles with a positive real part, since the (real-valued) poles of the elements of Σ^{-1} are located in the closed left s-half-plane. In the neighborhood of $s=0$, we have $R_\ell(s) \sim (2\ell)!D^{\ell}/(s/c)^{\ell+1}$. The long-time behavior of $R_\ell(t)$ is due to this contribution. Taking the inverse Laplace transform leads in TD to

$$R_\ell(t) \sim c\frac{(2\ell)!}{\ell!}(Dct)^{\ell} \quad \text{as}\, t\to\infty.$$

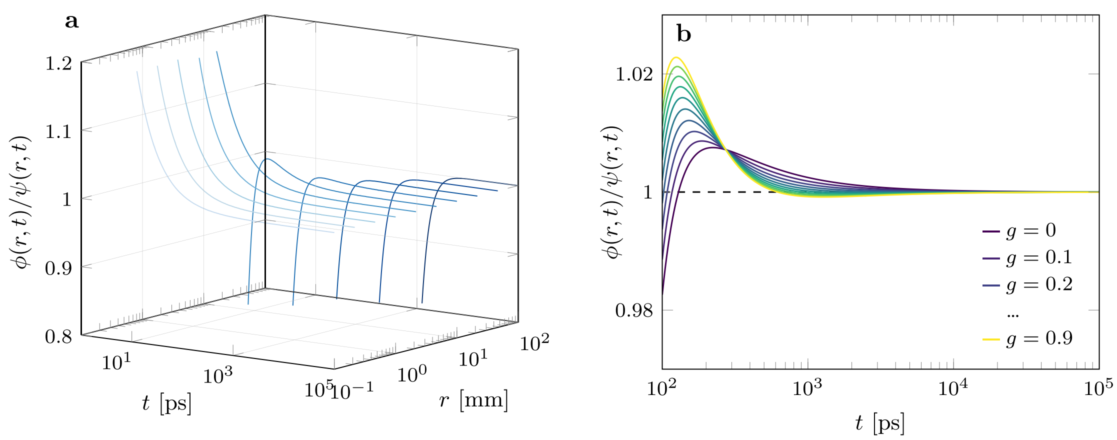

Figure 1. Time-domain convergence of the RTE fluence to the DE candidate with absorption-independent diffusion coefficient. (a) Ratio $\phi(r,t)/\psi(r,t)$ as a function of time and distance for isotropic scattering, computed for $\mu_a = 0.01\,\mathrm{mm}^{-1}$ and $\mu_s = 1\,\mathrm{mm}^{-1}$. All curves converge pointwise to 1 for $t \to \infty$ irrespective of the distance r. (b) Convergence to 1 is preserved, as expected, also in the anisotropic scattering case for $g \in [0, 0.9]$ (shown illustratively for $r = 10\,\mathrm{mm}$).

These moments are unique and belong to the Gaussian function $f(r,t) = c\mathrm{e}^{-r^2/(4Dct)}/(4\pi Dct)^{3/2}$, because

$$c\frac{(2\ell)!}{\ell!}(Dct)^\ell = \frac{4\pi}{2\ell+1}\int_0^\infty r^{2\ell} f(r,t) r^2 \,\mathrm{d}r.$$

Finally, by reconsidering the absorbing factor $\mathrm{e}^{-\mu_a ct}$, we obtain:

$$\Phi(r,t) \sim \mathrm{e}^{-\mu_a ct} f(r,t) = \phi(r,t) = \frac{c\mathrm{e}^{-\mu_a ct}}{(4\pi Dct)^{3/2}}\mathrm{e}^{-r^2/(4Dct)} = \psi(r,t) \quad \text{as}\, t \to \infty,$$

with the diffusion coefficient $D := 1/(3\mu_s')$. In view of (4), this establishes the '$\Longleftarrow$' implication. The reverse implication '$\Longrightarrow$' can again be proved by contraposition. As in the previous case, using the parametrized diffusion coefficient, one obtains

$$\kappa = \frac{1}{3}\frac{1}{a\mu_a + \mu_s'} \quad \Longrightarrow \quad \lim_{t\to\infty}\frac{\phi(r,t)}{\tilde{\psi}(r,t)} = \left(\frac{\mu_s'}{a\mu_a + \mu_s'}\right)^{3/2} < 1,$$

showing that a finite discrepancy would remain at all times. We thus arrive at the same conclusion as in the case of isotropic scattering.

2.3. Summary for the infinite time-asymptotic limit

An overview of the behavior of the time-dependent limit in a 3D infinite medium is shown in figure 1(a), where the ratio $\phi(r,t)/\psi(r,t)$ is plotted as a function of time and distance for a representative pair of values $\mu_a = 0.01\,\mathrm{mm}^{-1}$ and $\mu_s = 1\,\mathrm{mm}^{-1}$ for isotropic scattering. Figure 1(b) shows that the convergence to 1 is preserved also in the anisotropic scattering case as expected, for $g \in [0, 0.9]$ where a Henyey–Greenstein model was used for the scattering phase function. In all cases, a time-asymptotic convergence to 1 is observed regardless of the distance r from the source and of g. For $g > 0$, the calculation of the RTE fluence was done using (18), while for $g = 0$ the calculation can be performed using equivalently (18) or (6), with results shown illustratively for the case of $r = 10\,\mathrm{mm}$. Figure 2(a) displays the ratio $\phi(r,t)/\tilde{\psi}(r,t)$ versus t for the case $r = 10\,\mathrm{mm}$ and $a \in [0, 1]$, showing the general behavior for typical diffusion coefficients of the form expressed by (3). As we demonstrated, the correct convergence is obtained only in the case $a = 0$. Finally, figure 2(b) shows the limit of the ratio $\phi(r,t)/\tilde{\psi}(r,t)$ versus μ_a/μ_s for the isotropic case, showing that setting $a = 0$ ensures convergence regardless of the value of μ_a/μ_s.

With the above derivation, we have provided a more physically based alternative to the typical textbook derivation of the DE from the RTE. Our approach started from the requirement that diffusion must represent the infinite-time asymptotic limit of radiative transfer, which allowed us to derive a correspondence criterion between the DE and the RTE in the TD that should take precedence over the

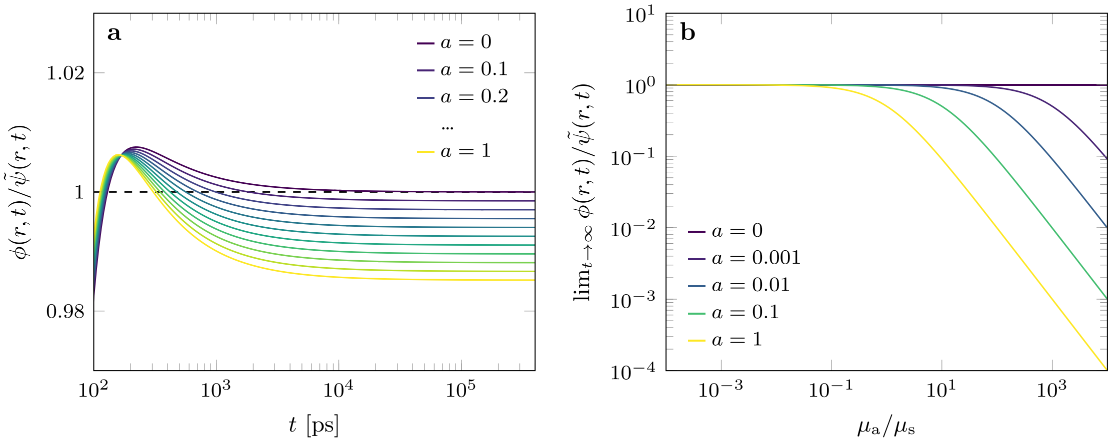

Figure 2. Effect of using a parametrized TD diffusion coefficient in the DE candidate. (a) Introducing any value of $a \neq 0$ in $\tilde{\psi}$ shifts the infinite-time limit below 1 (shown illustratively for $r = 10$ mm). (b) Dependence of the infinite-time asymptotic limit on the μ_a/μ_s ratio for different values of a in the isotropic scattering case.

approximations introduced in the classical derivation of the DE. To the best of our knowledge, this relevant equivalence was never recognized nor exploited in these terms, showing that using an absorption-dependent diffusion coefficient leads to a finite discrepancy that is not remedied even in the infinite-time asymptotic limit. Any absorption-dependent coefficient of the form (3) leaves a finite asymptotic discrepancy, and therefore a systematic long-time fluence error, even before finite-geometry or instrumental effects are considered.

3. Infinite space-asymptotic limit

We now apply the same asymptotic-consistency criterion to the steady-state, or CW, Green's function. The relevant limit is no longer $t \to \infty$ at fixed position, but $r \to \infty$ after integration over all times. We therefore start from the infinite-medium CW RTE Green's functions for isotropic (section 3.1) and anisotropic (section 3.2) scattering and compare their large-distance asymptotics with the scalar DE Green's function.

The Green's function for the DE fluence in an infinite medium is one of the most widely used expressions in diffuse optical transport:

$$\Phi_{\mathrm{DE}}(r) = \frac{\mathrm{e}^{-\mu_{\mathrm{eff}} r}}{4\pi D r}, \tag{24}$$

where $\mu_{\mathrm{eff}} := \sqrt{\mu_a/D}$ is the effective attenuation coefficient. Throughout this section, $\tilde{\psi}$ denotes the DE-shaped expression obtained from (24) with an arbitrary value of the parameter a in (3). When a is chosen to match the dominant RTE pole, we denote this value by a^* and the corresponding DE-shaped surrogate by ψ^*. The corresponding scalar diffusion coefficient is denoted by D^*, while D_{res} denotes the generally different scalar coefficient that would be required to match the dominant residue. The distinction between the two coefficients is a key feature of the CW analysis: a scalar diffusion Green's function ties decay length and amplitude to the same coefficient, which is incompatible with the asymptotic limit of the RTE.

In the next sections 3.1 and 3.2, the Green's functions of the RTE in an infinite medium for isotropic and anisotropic scattering are reported and their asymptotic behavior is used to evaluate the large-distance ratio between RTE and DE solutions, as summarized in section 3.4.

3.1. Isotropic scattering

The infinite-space fluence in an isotropically scattering medium can be derived without recourse to the P_N method. Starting from the derivations outlined by Case and Zweifel [1], one can obtain the following expression (see [39], equation (6.77)):

$$\phi(r) = \frac{\mu_t{}^3\lambda^2\left(1-\lambda^2\right)}{\mu_t\lambda^2-\mu_a}\frac{\mathrm{e}^{-\mu_t\lambda r}}{2\pi\mu_s r} + \frac{1}{4\pi r}\int_{\mu_t}^{\infty}\frac{\mathrm{e}^{-\xi r}}{\left(1-\mu_s \operatorname{artanh}\left(\mu_t/\xi\right)/\xi\right)^2 + \left[\mu_s\pi/(2\xi)\right]^2}\,\mathrm{d}\xi, \tag{25}$$

where $\mu_\mathrm{t} := \mu_\mathrm{a} + \mu_\mathrm{s}$. Here, the corresponding eigenvalue $\lambda \in [0,1)$ must be found as solution of the equation

$$\frac{\operatorname{artanh}\lambda}{\lambda} = \frac{\mu_\mathrm{t}}{\mu_\mathrm{s}} = 1 + \frac{\mu_\mathrm{a}}{\mu_\mathrm{s}}. \tag{26}$$

For λ near zero, a good initial guess (e.g. for Newton's method) is given by $\lambda_0 = \sqrt{3\mu_\mathrm{a}/\mu_\mathrm{t}}$, which is due to the fact that $\frac{1}{\lambda}\operatorname{artanh}\lambda = 3/(3-\lambda^2) + \mathcal{O}(\lambda^4)$ as $\lambda \to 0$. In the following, we show that in the case of $\mu_\mathrm{a} > 0$, no diffusion coefficient $D > 0$ exists for obtaining $\lim_{r\to\infty}\phi(r)/\psi(r) = 1$. For this task, it is sufficient to consider $\lambda \in (0,1)$, because $\lambda = 0$ corresponds to $\mu_\mathrm{a} = 0$. The special case of a non-absorbing medium will be addressed at the end of this subsection. We first need to identify the leading term at large distances. It corresponds with the first term of (25), which can be seen by the estimate of the second term

$$\begin{aligned} I(r) &:= \frac{1}{4\pi r}\int_{\mu_\mathrm{t}}^{\infty} \frac{\mathrm{e}^{-\xi r}}{\left(1-\mu_\mathrm{s}\operatorname{artanh}(\mu_\mathrm{t}/\xi)/\xi\right)^2 + \left[\mu_\mathrm{s}\pi/(2\xi)\right]^2}\,\mathrm{d}\xi \leqslant \frac{1}{{\mu_\mathrm{s}}^2\pi^3 r}\int_{\mu_\mathrm{t}}^{\infty}\xi^2\mathrm{e}^{-\xi r}\,\mathrm{d}\xi \\ &= \frac{1}{{\mu_\mathrm{s}}^2\pi^3}\,\frac{2+2\mu_\mathrm{t}r+(\mu_\mathrm{t}r)^2}{r^4}\mathrm{e}^{-\mu_\mathrm{t}r} \sim \frac{\mathrm{e}^{-\mu_\mathrm{t}r}}{r^2} \quad \text{as}\, r\to\infty. \end{aligned} \tag{27}$$

Since $\lambda \in (0,1)$, we have $\mathrm{e}^{-\mu_\mathrm{t}r} < \mathrm{e}^{-\mu_\mathrm{t}\lambda r}$ for all $r > 0$ so that the leading term of (25) at large distances is indeed the first one, i.e.

$$\phi(r) \sim \frac{{\mu_\mathrm{t}}^3\lambda^2\left(1-\lambda^2\right)}{\mu_\mathrm{t}\lambda^2-\mu_\mathrm{a}}\,\frac{\mathrm{e}^{-\mu_\mathrm{t}\lambda r}}{2\pi\mu_\mathrm{s}r} \quad \text{as}\, r\to\infty. \tag{28}$$

In trying to match the Green's function of the DE (24) to this asymptotic transport fluence, the minimal requirement is to reproduce the same exponential decay. This imposes the condition

$$\sqrt{\frac{\mu_\mathrm{a}}{D}} = \mu_\mathrm{t}\lambda \quad \Longleftrightarrow \quad D = \frac{\mu_\mathrm{a}}{(\mu_\mathrm{t}\lambda)^2} \equiv D^*, \tag{29}$$

where the eigenvalue λ is determined by (26). To highlight the discrepancy in the asymptotic regime with respect to the RTE for any given diffusion Green's function, we explicitly demonstrate this mismatch when using the adapted decay rate (29). The function $\psi(r) = \mathrm{e}^{-\mu_\mathrm{t}\lambda r}/(4\pi Dr)$ solves the classical DE $-D\nabla^2\psi + \mu_\mathrm{a}\psi = \delta_0$, where δ_0 is the Dirac delta at the source position. Consequently, the asymptotic ratio $\phi(r)/\psi(r)$ can be calculated:

$$\lim_{r\to\infty}\frac{\phi(r)}{\psi(r)} = \frac{2\mu_\mathrm{a}\mu_\mathrm{t}}{\mu_\mathrm{s}}\,\frac{1-\lambda^2}{\mu_\mathrm{t}\lambda^2-\mu_\mathrm{a}} = \frac{2q(q-1)\left(1-\lambda^2\right)}{1-(1-\lambda^2)q} = \frac{2q^2-2q}{1/(1-\lambda^2)-q}, \tag{30}$$

where $q := \mu_\mathrm{t}/\mu_\mathrm{s} = \frac{1}{\lambda}\operatorname{artanh}\lambda$. In evaluating this limit, we have used $\lim_{r\to\infty} I(r)/\psi(r) = 0$, which is because

$$0 \leqslant \frac{I(r)}{\psi(r)} \leqslant \frac{4D}{(\mu_\mathrm{s}\pi)^2}\,\frac{2+2\mu_\mathrm{t}r+(\mu_\mathrm{t}r)^2}{r^3}\mathrm{e}^{-\mu_\mathrm{t}(1-\lambda)r} \longrightarrow 0 \quad \text{as}\, r\to\infty. \tag{31}$$

In view of (30), we note that the ratio of two positive functions remains positive, which implies that $1/(1-\lambda^2) - q > 0$. This information will be used in (32). We proceed by introducing

$$\begin{aligned} H(\lambda) &:= \frac{1}{1-\lambda^2} + \frac{\operatorname{artanh}\lambda}{\lambda} - 2\left(\frac{\operatorname{artanh}\lambda}{\lambda}\right)^2 \\ &= \sum_{\ell=0}^{\infty}\lambda^{2\ell} + \sum_{\ell=0}^{\infty}\frac{\lambda^{2\ell}}{2\ell+1} - 2\sum_{\ell=0}^{\infty}\left(\sum_{\mu=0}^{\ell}\frac{1}{2\mu+1}\,\frac{1}{2\ell-2\mu+1}\right)\lambda^{2\ell} \\ &= \sum_{\ell=2}^{\infty} c_{2\ell}\lambda^{2\ell} \quad \text{for}\, \lambda \in (0,1). \end{aligned}$$

Note that all the series appearing here converge on $(0,1)$. The resulting expansion coefficients become

$$c_{2\ell} = 1 + \frac{1}{2\ell+1} - \frac{2}{\ell+1}\sum_{\mu=0}^{\ell}\frac{1}{2\mu+1}, \quad \ell \geqslant 2,$$

where we have used

$$\sum_{\mu=0}^{\ell}\frac{1}{2\mu+1}\frac{1}{2\ell-2\mu+1}=\frac{1}{\ell+1}\sum_{\mu=0}^{\ell}\frac{1}{2\mu+1}.$$

These coefficients are strictly positive, which is because

$$\begin{aligned}c_{2\ell}&=1+\frac{1}{2\ell+1}-\frac{2}{\ell+1}\sum_{\mu=0}^{\ell}\frac{1}{2\mu+1}>1+\frac{1}{2\ell+1}-\frac{2}{\ell+1}-\frac{2}{\ell+1}\sum_{\mu=1}^{\ell}\frac{1}{3}\\&=1+\frac{1}{2\ell+1}-\frac{2}{\ell+1}-\frac{2}{3}\frac{\ell}{\ell+1}=\frac{2}{3}\frac{\ell(\ell-1)}{(\ell+1)(2\ell+1)}>0,\end{aligned}$$

for all $\ell\geqslant 2$. Thus, the function H defined on $(0,1)$ is also strictly positive, which leads, recalling (30), to the following condition

$$H(\lambda)=\frac{1}{1-\lambda^2}+q-2q^2>0\quad\iff\quad\frac{2q^2-2q}{1/(1-\lambda^2)-q}<1. \tag{32}$$

This shows that, if $\mu_a>0$ and $D=\mu_a/(\mu_t\lambda)^2$, we have $\lim_{r\to\infty}\phi(r)/\psi(r)<1$. For any other value of $D>0$, the exponential decay rate of the diffusion Green's function differs from the RTE rate $\mu_t\lambda$, so the same ratio either vanishes or diverges exponentially. Thus, no scalar diffusion coefficient can produce $\lim_{r\to\infty}\phi(r)/\psi(r)=1$ for $\mu_a>0$.

As a byproduct, the pole-matching condition (29) determines the corresponding value of a within the parametrized family $D=[3(\mu_s+a\mu_a)]^{-1}$. Specifically,

$$\frac{1}{3(\mu_s+a^*\mu_a)}=D^*\quad\Longrightarrow\quad a^*=\frac{(\mu_t\lambda)^2}{3\mu_a{}^2}-\frac{\mu_s}{\mu_a}.$$

Then, by using D^* inside the DE solution, we obtain the surrogate solution ψ^* that best reproduces the RTE decay, i.e.

$$\psi^*(r)=\frac{1}{4\pi D^*r}\mathrm{e}^{-\sqrt{\mu_a/D^*}r}. \tag{33}$$

As an example, for $q=\mu_t/\mu_s=1.01$, we get $\lambda\approx 0.171661779$ and hence $a^*\approx 0.200228571$.

We conclude this subsection by examining the asymptotic behavior of the transport theory fluence in the non-absorbing medium. In this case, the leading term is still given by (28), where we take the limit $\mu_a\to 0$. In this situation, we again can use $\lambda\approx\sqrt{3\mu_a/\mu_t}$, which results in

$$\phi(r)\sim\frac{\mu_t{}^3\lambda^2\left(1-\lambda^2\right)}{\mu_t\lambda^2-\mu_a}\frac{\mathrm{e}^{-\mu_t\lambda r}}{2\pi\mu_s r}=\frac{3\mu_t{}^2}{2}\frac{1-3\mu_a/\mu_t}{2\pi\mu_s r}\mathrm{e}^{-\mu_t\sqrt{3\mu_a/\mu_t}r}\longrightarrow\frac{1}{4\pi Dr}\quad\text{as }\mu_a\to 0,$$

with $D=1/(3\mu_s)$ as the (standard) diffusion coefficient for non-absorbing media. Thus, in contrast to the case $\mu_a>0$, the CW fluence predicted by transport theory agrees at infinite radial distances (in the absence of absorption) with that one approximated by the classical (non-absorbing) DE. We note that in this situation, the DE takes the form of Poisson's equation.

3.2. Anisotropic scattering

In the case of anisotropic scattering, the infinite-space fluence in the steady-state domain can be expressed as a superposition of diffusion-like Green's functions [40]:

$$\Phi(r)=\sum_{i=1}^{\frac{N+1}{2}}A_i\frac{\mathrm{e}^{-\nu_i r}}{4\pi r}, \tag{34}$$

with coefficients A_i and attenuation rates ν_i. The solution is based on the spherical harmonics equations (P_N approximation) and by selecting a sufficiently large number of terms N we can guarantee convergence to the exact RTE. A detailed derivation of this expression and the definition of the required coefficients A_i and ν_i can be found in [40, equations (15) and (16)], and a numerical implementation of these functions is available as supplemental code.

The expression in (34) provides a direct way to identify the dominant asymptotic term also for anisotropic scattering, once the P_N solution is evaluated at a sufficiently converged order N. After ordering the positive attenuation coefficients so that $\nu_1 \leqslant \nu_2 \leqslant \cdots$, the large-distance behavior is

$$\Phi(r) \sim A_1 \frac{\mathrm{e}^{-\nu_1 r}}{4\pi r} \quad \text{as r} \to \infty.$$

Matching the dominant exponential decay requires

$$D^* = \frac{\mu_\mathrm{a}}{\nu_1^2},$$

whereas matching the dominant residue would require $D_\mathrm{res} = 1/A_1$. Therefore, the same pole–residue compatibility condition identified explicitly in the isotropic case extends naturally to the anisotropic calculation: a scalar diffusion Green's function can match both asymptotic quantities only if $D^* = D_\mathrm{res}$, which occurs only for $\mu_\mathrm{a} = 0$.

3.3. Finite scattering orders and the CW asymptotic tail

The pole–residue obstruction also clarifies a common misconception regarding the role of early, non-diffusive light. Since the CW Green's function is the time integral of the TD Green's function, one may argue that the CW discrepancy is caused by the ballistic and low-order scattering terms that are included in the time integral before the TD solution has reached its diffusive limit. This interpretation, however, is not valid in the large-distance asymptotic regime. To see this, let Ψ_n denote the CW contribution obtained after suppressing all terms with scattering order below n, with $n = 0$ corresponding to the complete fluence. In 3D Fourier space, $\mathcal{F}\Psi_n = \hat{\Phi}_n$ can be written as

$$\hat{\Phi}_n(k) = \hat{\phi}(k) - \sum_{\ell=0}^{n-1} \mu_\mathrm{s}^\ell \left(\hat{\phi}_0(k)\right)^{\ell+1} = \mu_\mathrm{s}^n \frac{\left(\frac{\arctan(k/\mu_\mathrm{t})}{k}\right)^{n+1}}{1 - \mu_\mathrm{s}\frac{\arctan(k/\mu_\mathrm{t})}{k}}, \tag{35}$$

where $\hat{\phi}_0(k) = \arctan(k/\mu_\mathrm{t})/k$ is the transformed ballistic part and $\hat{\phi}$ is the Fourier transform of the complete fluence (25) [8, chapter 5, section 5.2]. For $n = 0$, (35) is just the Fourier transform of the complete fluence namely $\hat{\Psi}_0 = \hat{\phi}$. Equivalently, $\hat{\Phi}_n = (\mu_\mathrm{s}\hat{\phi}_0)^n\hat{\phi}$. In real space this corresponds to convolving the complete fluence ϕ with the ballistic kernel $\mu_\mathrm{s}\phi_0$, n times, over $\mathbb{R}^3$. At $k = 0$, this gives

$$\hat{\Phi}_n(0) = \left(\frac{\mu_\mathrm{s}}{\mu_\mathrm{t}}\right)^n \frac{1}{\mu_\mathrm{a}} = \int_{\mathbb{R}^3} \Psi_n(\mathbf{r})\,\mathrm{d}\mathbf{r},$$

so, for $n > 0$, Ψ_n is not normalized as a unit-power source CW Green's function, i.e. its spatial integral on the whole volume is not 1. Essentially, Ψ_n represents the contribution to the fluence from light that has survived and undergone at least n scattering events. Re-normalizing it to unit injected power would multiply the far-field residue by $(\mu_\mathrm{t}/\mu_\mathrm{s})^n$ and would define a different conditional source ensemble. The key point for the present work is that the dominant CW pole is unchanged. The poles closest to the real axis remain located at $k = \pm\mathrm{i}\lambda\mu_\mathrm{t}$, independently of any fixed finite n, where λ solves (26). More importantly, the factor introduced by removing low-order scattering terms equals unity at the pole, because

$$\left(\mu_\mathrm{s}\hat{\phi}_0(k)\right)^n\Big|_{k=\mathrm{i}\lambda\mu_\mathrm{t}} = \left[\frac{\mu_\mathrm{s}}{\mu_\mathrm{t}}\frac{\operatorname{artanh}\lambda}{\lambda}\right]^n = 1.$$

Thus the leading residue is unchanged as well. Equivalently, evaluating the residue explicitly gives

$$\operatorname{Res}\left\{\hat{\Phi}_n(k)\,\mathrm{e}^{\mathrm{i}kr}, k = \mathrm{i}\lambda\mu_\mathrm{t}\right\} = \frac{{\mu_\mathrm{t}}^2}{\mathrm{i}\mu_\mathrm{s}} \frac{\lambda\left(1-\lambda^2\right)}{\mu_\mathrm{t}\lambda^2 - \mu_\mathrm{a}} \mathrm{e}^{-\mu_\mathrm{t}\lambda r}, \tag{36}$$

which is independent of n. Applying the inverse spherically symmetric Fourier transform then recovers the same leading term as in (28).

Therefore, suppressing any fixed finite number of low-scattering contributions changes the finite-distance CW fluence but not its dominant large-distance asymptotic term, which is an intrinsic property of the dominant spatial pole and residue of the transport resolvent.

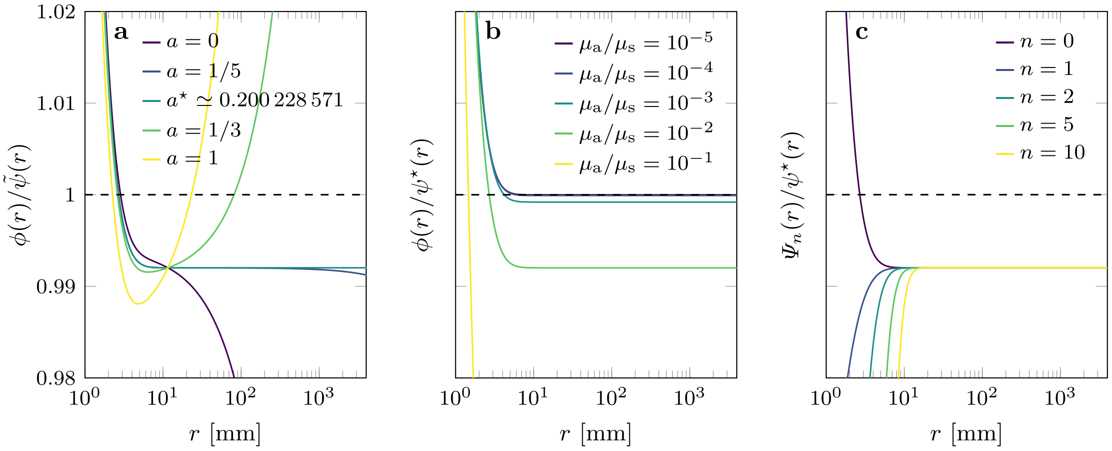

Figure 3. Ratio between the RTE and DE candidate solutions. (a) Ratio $\phi(r)/\tilde{\psi}(r)$ as a function of distance, computed for $\mu_a = 0.01\,\mathrm{mm}^{-1}$ and $\mu_s = 1\,\mathrm{mm}^{-1}$ and isotropic scattering ($g = 0$). For a specific pole-matched value of a close to $1/5$, the ratio converges to a finite stable limit. (b) A different pole-matched value a^* is required for each value of μ_a/μ_s. Taking $a^* = 1/5 + \epsilon$, we find $\epsilon \simeq 2.287 \times 10^{-7}, 2.286 \times 10^{-6}, 2.286 \times 10^{-5}, 2.286 \times 10^{-4}, 2.285 \times 10^{-3}$ for $\mu_a/\mu_s = 1 \times 10^{-5}, 1 \times 10^{-4}, 1 \times 10^{-3}, 1 \times 10^{-2}, 1 \times 10^{-1}$, respectively. (c) The same asymptotic ratio plotted in (b) for $\mu_a/\mu_s = \times 10^{-2}$ is shown after suppressing all scattering contributions below n.

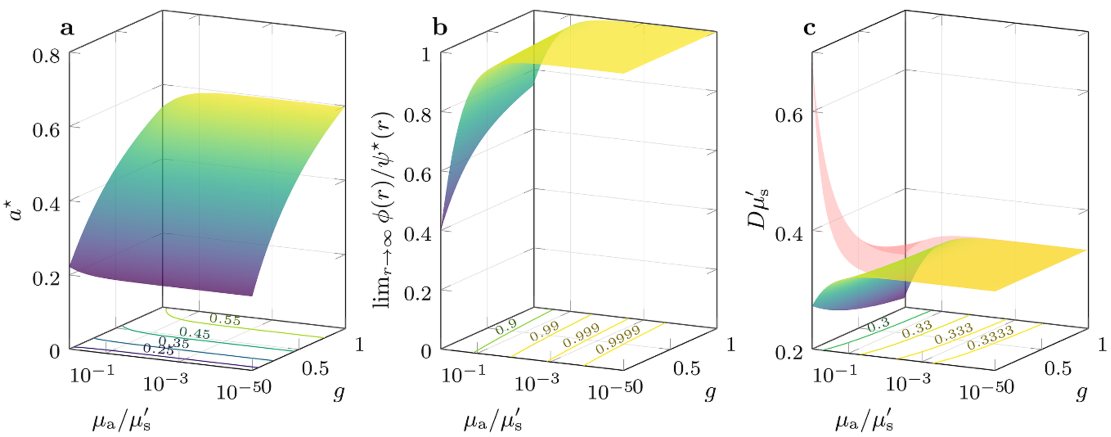

Figure 4. CW asymptotic quantities in the anisotropic case. (a) Similar considerations hold also in the anisotropic scattering case, with pole-matched a^* values spanning from roughly 0.2 to 0.6 for g values in the range $0 \leqslant g < 1$ (data calculated for $\mu_s' = 1\,\mathrm{mm}^{-1}$). (b) Value of the asymptotic ratio obtained using the pole-matched a^* value for each combination of parameters. With decreasing albedo, the asymptotic ratio remains below unity and decreases smoothly over the plotted range. (c) The two scalar diffusion coefficients required to match the dominant RTE pole, D^*, or the corresponding asymptotic residue, D_{res}, remain distinct for the same combinations of optical parameters. Selected contour lines are plotted below the surfaces.

3.4. Summary of the infinite radial-asymptotic limit

Using the previously reported steady-state solutions, we can study the convergence of the CW DE solution to the CW RTE solution by calculating the fluence ratio (RTE/DE) as a function of source–detector distance r. Figure 3 summarizes the isotropic case and highlights three distinct aspects of the CW obstruction: the sensitivity to the scalar coefficient D, the approach to the weak-absorption limit, and the invariance of the dominant asymptotic ratio after the suppression of finitely many low-scattering contributions.

In particular, figure 3(a) uses $\tilde{\psi}$ to denote the DE-shaped expression with a generic value of a, while figures 3(b), (c) and figure 4 use ψ^* for the pole-matched choice a^*. In all cases, $\phi(r)$ represents the corresponding RTE solution ((25) or (34) for isotropic or anisotropic scattering, respectively). Looking at the illustrative results for $\mu_a = 0.01\,\mathrm{mm}^{-1}$ and $\mu_s = 1\,\mathrm{mm}^{-1}$ with isotropic scattering, it can be seen that the stability of the space-asymptotic ratio depends critically on the diffusion coefficient D through the value of the parameter a. For this specific combination of optical properties, a unique value

$a^* \simeq 0.200\,228\,571\,055\,617$ exists after matching the dominant RTE pole such that the $\phi(r)/\psi^*(r)$ does not exponentially diverge or collapse to zero.

In the limit of vanishing absorption, for the isotropic scattering case, the value of a^* converges to $1/5$ as predicted by transport theory [24, 32, 41], and the asymptotic ratio converges toward 1. The convergence behavior is illustrated in figure 3(b), showing the limits for different values of μ_a/μ_s obtained when using the specific pole-matched values a^* for each configuration. Figure 3(c) complements this result by showing that the same asymptotic ratio is recovered even after suppressing any fixed finite number of low-scattering contributions. This confirms that the CW discrepancy is not a finite-order contamination by ballistic or few-scattering light, but a property of the dominant spatial mode itself.

The unique value of a^* determining a finite limiting value is found to depend even more strongly on the scattering asymmetry g, as shown in figure 4(a) for the Henyey–Greenstein case. With the dominant-pole calculation, retrieved values vary smoothly over the investigated range and span approximately between $0.2 \leqslant a^* < 0.6$ for $0 \leqslant g < 1$, as qualitatively reported in some previous works [24, 30, 41].

Figure 4(b) shows the corresponding $\lim_{r\to\infty} \phi(r)/\psi^*(r)$, which is always found to be strictly below 1, decreasing smoothly as absorption increases over the plotted range. Figure 4(c) provides a parametrization-independent view of the same CW obstruction: matching the dominant exponential decay and matching the dominant prefactor impose two different scalar diffusion coefficients, denoted D^* and D_{res}, respectively.

In the same spirit of the time-domain analysis, diffusive propagation under steady state conditions implies that the DE and RTE solutions should coincide asymptotically for $r \to \infty$. Our analysis shows that this condition is verified rigorously only in the very special case of a non-absorbing medium with isotropic scattering—i.e. the only case where all expressions for the diffusion coefficient coincide trivially.

For any general case with $\mu_a > 0$, matching the leading CW decay fixes a specific value of $a^*(\mu_a, g)$, determined by the dominant RTE pole. Most notably, even when using such specific value, the DE is never found to converge exactly to the asymptotic RTE fluence, in stark contrast with the time-domain picture where exact convergence is always observed for any degree of absorption and scattering anisotropy.

The previous asymptotic results identify which diffusion coefficient is mathematically consistent, but they do not by themselves quantify the bias that may be incurred in a finite-window retrieval. To provide an order-of-magnitude estimate, figure 5 compares the error in the absorption coefficient retrieved by fitting DE Green's functions to RTE data in an infinite homogeneous medium. Following a common situation in applications, we retrieve an unknown absorption coefficient while assuming known the value for the reduced scattering coefficient. The same fitting protocol is used in both TD and CW domain, keeping the overall amplitude as an additional free parameter to mimic measurements in arbitrary units. Given the assumptions of perfect knowledge on μ_s' and noiseless infinite medium with no boundaries or refractive-index heterogeneities, this comparison should be read as an intrinsic model bias rather than a comprehensive experimental error budget applicable to arbitrary configurations. In realistic finite samples, additional sources of bias may either aggravate or compensate the intrinsic bias shown here, and even in the ideal infinite-medium setting, the retrieval error depends on additional factors such as the source–detector separation, the fitting window and the residual model. Hence, the values in figure 5 quantify the scale of the avoidable bias inflicted by using an asymptotically inconsistent diffusion coefficient. In the TD, the correct asymptotic coefficient $D = 1/(3\mu_s')$, corresponding to $a = 0$, gives a smaller absorption bias than the canonical coefficient $D = 1/[3(\mu_s' + \mu_a)]$ in the TD retrieval of figure 5(a), where the fitting window is started at the time of maximum fluence. Especially at low albedo, a residual error can be seen also in the $a = 0$ case, because the finite fitting window is not yet in the late-time regime. Indeed, when the fit is slightly shifted farther into the tail, as in figure 5(b), the $a = 0$ bias stays small or decreases substantially, whereas the canonical $a = 1$ bias is only weakly reduced and remains finite, as expected from our analytical demonstration. The CW domain case displays the same issue even more directly. Figure 5(c) compares the canonical parametrization $a = 1$ with the pole-matched coefficient D^*, which reproduces the dominant RTE attenuation length. As anticipated by the CW pole analysis, the pole-matched model retrieves μ_a essentially without bias in this fitting scenario, whereas the canonical parametrization produces a systematic absorption bias that increases with absorption. At optical properties of $\mu_a/\mu_s' = 0.1$ and $g = 0.9$ typical of certain biomedical applications, using the DE formulation with $a = 1$ results in errors of several percent points, compared to the basically exact absorption retrieval obtained with the $a = 0$ or a^* formulation in the TD and CW domain, respectively.

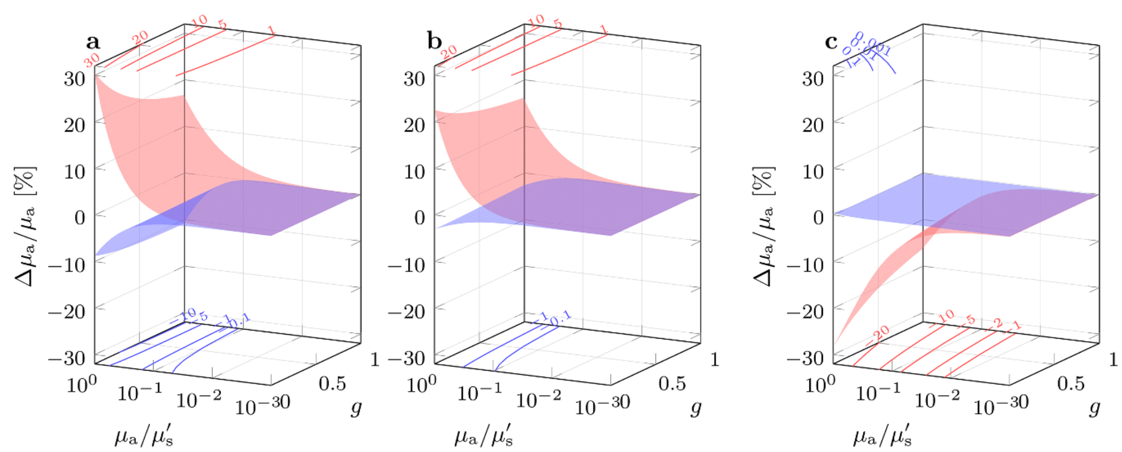

Figure 5. Bias in the absorption coefficient retrieved by fitting DE Green's functions to RTE data with known μ_s' and floated amplitude. The blue branch denotes the TD-asymptotic choice $a = 0$ in panels (a), (b), and the CW pole-matched choice a^* in panel (c); the red branch denotes the canonical parametrization $a = 1$. All fits are performed in logarithmic scale over 100 data points spanning a finite dynamic range of 10^{-3}. (a) Retrieved μ_a bias for the time-resolved fluence at $r = 10$ mm. For each configuration, the fitting range starts from the time where $\Phi(r,t)$ reaches its peak amplitude, down to the time where it has decayed to 10^{-3} of its peak value. (b) Same as before, but with a fitting range starting from $1.5\times$ the peak time. (c) Retrieved μ_a bias for the steady-state fluence measured between $r = 10$ mm and a distance such that the fluence has decayed to 10^{-3} its value at 10 mm. Selected contour lines are projected below and above the surfaces for the blue and red branches, respectively.

4. Discussion

The analysis presented in section 2, and the results summarized in figure 1, establish the TD as the theoretical framework of preference in which the DE expresses its proper meaning as an asymptotic approximation to radiative transfer. With increasing time, the diffusion solution converges exactly to the RTE *if and only if* the diffusion coefficient D is taken to be independent of μ_a, thus preserving also a fundamental scaling relation of the RTE. This convergence holds in the asymptotic limit for arbitrary scattering anisotropy and, more generally, for arbitrary scattering phase functions. Therefore, the TD should be regarded as the reference regime for defining light diffusion from radiative transfer.

The situation is fundamentally different in the steady-state domain. As shown in figure 4, no choice of D can yield exact convergence between the DE and the RTE in the infinite distance limit when $\mu_a > 0$. This irreducible discrepancy implies that the steady-state DE cannot be regarded as an asymptotic limit of radiative transfer under general conditions. A quantitative agreement is observed only for the special case of a non-absorbing medium ($\mu_a = 0$), where the Green's function of the DE becomes identical to the Green's function of the Poisson equation, which is exact in the asymptotic regime of non-absorbing media. This mathematical exception, however, has little relevance to real world applications, where absorption is always present to some extent.

From an analytical standpoint, given the functional dependence of the DE solution (24), this discrepancy is rooted in the fact that the coefficient D cannot alter the total absorbed power within the medium [8, 42]. This explains why, due to this constraint, it is only possible to find a parametrization of D ensuring proportionality (same asymptotic decay rate) rather than exact coincidence of the asymptotic fluence between the RTE and the DE. Equivalently, a pure diffusion Green's function cannot simultaneously match the RTE attenuation length, dominant amplitude, and unit-source normalization. This impossibility is reflected in the violation of the so-called similarity relation [8, 10, 43, 44], which states that diffusive light transport should not retain a memory of single-scattering properties (μ_s and g) after sufficiently many scattering events. In the TD, similarity is recovered exactly in the long-time limit, irrespective of absorption and scattering anisotropy. In the steady state, by contrast, the asymptotic fluence generally retains a dependence on μ_a, μ_s, and g even at infinite distance. As a result, two media with identical μ_s' but different g can yield different steady-state asymptotic fluence values, raising the question of whether steady-state diffusion constitutes a physically self-consistent concept.

This consideration stands in contrast with much of the previous literature, starting with the framework laid out by Aronson and Corngold [24] and inspired by the fundamental work from Case and Zweifel [1], where a steady-state perspective is dogmatically adopted as the basis for defining D. As such, a dependence on either absorption or g was not interpreted as a failure of the diffusive approximation, but rather treated as one of its characteristics. In this work, rather than postulating *a priori* the superiority of one domain over the others, we simply require that diffusion emerges as the asymptotic limit of the RTE, and find that this condition cannot be satisfied in the CW regime.

Previous studies had already shown that a suitably parametrized D can qualitatively match the asymptotic decay rate of the RTE fluence [1, 24, 28, 30], but disregarded the fact that even a pole-matched expression tailored to each combination of optical parameters fails to reproduce the correct asymptotic limit of the steady-state RTE in absorbing media. This irreducible mismatch remained overlooked or undetected in earlier numerical comparisons, likely because the discrepancies become arbitrarily small as μ_a tends to zero, and thus were hidden by the intrinsic noise of Monte Carlo simulations [8] or by a larger attention paid to ensuring agreement close to the source or near boundaries [25, 45].

A first resolution of the apparent TD–CW discrepancy was given by Pierrat *et al* [9], who used a modal analysis of the RTE to show that the dynamic diffusion coefficient is the random-walk value $D = c/(3\mu_s')$, independent of absorption, whereas the steady-state coefficient is associated with the dominant spatial eigenvalue of the transport problem. What remained unclear in that interpretation, however, is that the two coefficients do not have the same asymptotic status. In the TD, the coefficient $D = 1/(3\mu_s')$ gives the leading Green's function itself. In the CW domain, the eigenvalue-based coefficient fixes only the dominant exponential decay, resulting in a different amplitude, or source normalization.

To the best of our knowledge, this irreducible discrepancy was never identified in the (rather vast) literature discussing possible definitions of the diffusion coefficient [1–7, 9, 24, 26–30, 44–50]. Conversely, even in the presence of diverging views on the topic, previous works generally treated both the TD and CW asymptotic propagation regimes as equally classifiable within a diffusion framework.

The pole-matching choice of D in the CW regime, expressed by selecting a^*, leads to the DE-shaped surrogate ψ^*, which reproduces the RTE decay but does not correspond to a proper diffusion process. Its dependence on single-scattering properties suggests that it should be best interpreted as an approximate radiative-transport surrogate that takes the same formal structure as the DE solution, without being an actual solution. This observation aligns with earlier attempts to develop 'improved' solutions of the DE [32, 51–53], including improvements for the calculation of the photon flux [54]. Compared to these expressions, the pole-matched surrogate ψ^* determined here is superior in the limited sense that it matches the asymptotic decay rate of the RTE at infinite radial distance, and it also includes the previously unaddressed anisotropic scattering case [32, 51–53].

A final theoretical point concerns the relation between TD and CW Green's functions through time integration. The naive argument that the same diffusion coefficient must apply in both domains because the CW solution is the time integral of the TD solution had already been criticized in previous works [9, 28]. In particular, Graaff and ten Bosch noted that the unscattered contribution alone cannot explain the far-field CW slope discrepancy, but still framed this issue as a failure of the Gaussian TD diffusion kernel as a route to the CW solution. Pierrat *et al* recovered the steady-state coefficient associated with the dominant RTE attenuation length, but did not address whether the resulting pole-matched coefficient defines a fully consistent scalar diffusion Green's function. The present analysis closes this interpretation gap by transforming the intuitive understanding—that the contribution of finite scattering order to the time integral vanishes in the spatial asymptotic limit—into a rigorous proof. The finite-scattering-order construction in section 3.3 shows that suppressing any fixed finite number of ballistic or few-scattering contributions leaves the dominant CW pole and residue unchanged. Thus the CW discrepancy is not a finite-order early-scattering contamination effect. In this sense, the absorption-dependent coefficient used in CW should be understood as an apparent pole-matching coefficient, not as a proper diffusion coefficient with the same status as the TD asymptotic coefficient which ensures the asymptotic correspondence between the DE and the RTE.

Beyond their theoretical meaning, these findings have practical implications whose impact should be assessed by a dedicated study. Most geometries of interest in diffuse optics, including the half-space, slab, and rectangular parallelepiped, derive their solutions from the infinite medium Green's function [8]. If the latter fails to correctly approximate the RTE in the steady-state regime, systematic errors will propagate to all derived solutions. At large distances, the pole-matched surrogate ψ^* provides minimal decay-rate deviations by incorporating the pole-matching dependence on μ_a and g into the expression of D. In many practical scenarios these parameters are not known *a priori*, leading to uncontrolled biases in the retrieval of optical parameters when using steady-state measurement data. For many biological tissues, where scattering anisotropy is typically $0.9 < g < 1$, the pole-matched values a^* mainly fall between 0.58 and 0.6 over a broad range of absorption levels. Thus, if one nevertheless uses CW diffusion for such media, this parametrization provides a least-inconsistent scalar choice, offering the best asymptotic attenuation rate correspondence with the exact RTE solution.

5. Conclusion

In this work, we have demonstrated that the TD provides the only strictly self-consistent framework for the application of the DE. In this domain, we have derived conclusively the correct expression (2) for the diffusion coefficient, confirming that it must be independent of absorption. This result is in full agreement with the fundamental scaling properties and asymptotic behavior of the RTE, guaranteeing exact convergence for all combinations of optical parameters.

In the steady state, even though it is possible to reproduce the dominant asymptotic decay of the RTE solution by introducing a parametrized diffusion coefficient (3) depending on both absorption and single-scattering asymmetry, this recovery remains only qualitative. A finite and irreducible discrepancy between the diffusion approximation and the RTE persists—even at infinite distance from the source—in all cases except the trivial non-absorbing one. This discrepancy reveals an oxymoron within the very idea of steady-state diffusion, which appears to either retain memory of single-scattering details, or diverge from the exact RTE.

These results carry important implications for the interpretation of experiments in diffuse optics. While CW measurement techniques are widely used and will remain relevant, these findings call for a reassessment of how diffusion theory is applied to their analysis. From a practical standpoint, this work enables the quantification of systematic errors introduced by the application of steady-state diffusion theory, including those affecting the estimation of the absorption coefficients and the scattering anisotropy factors whenever these parameters are not known *a priori*. At the same time, when these parameters are reasonably known, our framework provides an estimation of the least-incorrect value of a to be used in (3) for the analysis of large-distance CW measurements.

The results of this study introduce a surrogate CW solution ψ^* that, in the asymptotic spatial limit, reproduces the RTE attenuation length more accurately than previously proposed scalar DE-shaped approximations in the literature [32, 51–53]. This surrogate preserves the simplicity of the classical DE solution while incorporating the asymptotic transport behavior of the RTE, introducing a dependence on the single-scattering properties of the medium in its parametrization.

Finally, we have conclusively shown that under no circumstances should one use the 'canonical' expression (1), still in widespread use, for the diffusion coefficient. In the TD, this expression is incompatible with the exact absorption scaling and leaves a finite asymptotic error; in the CW domain, no combination of absorption or scattering asymmetry factor exists leading to a parameter $a^* = 1$ (or even $a^* > 0.6$). We therefore urge its discontinuation in the analysis of diffuse optical data, and advocate the time-domain formulation as the only theoretically sound reference regime for modeling light diffusion.

Acknowledgments

The authors thank Alessandro Torricelli for helpful comments and discussion.

Data availability statement

The data that support the findings of this study are openly available at the following URL/DOI: https://github.com/lpattelli/RTEsolutions [55].

Funding

F.M. acknowledges financial support by the European Union's—NextGenerationEU, National Recovery and Resilience Plan, PRIN 2022, DIRS, Missione 4 Componente 1, Grant Number: 2022EB4B7E [CUP B53D23002530006]. A.L. and A.K. acknowledge the financial support by the Deutsche Forschungsgemeinschaft (DFG, Grant Number KI 538/19-3 and Project Number 57 642 4554).

Author contributions

André Liemert 0000-0001-6326-1329
Conceptualization (equal), Data curation (equal), Formal analysis (equal), Investigation (equal), Methodology (equal), Software (equal), Supervision (equal), Validation (equal), Visualization (equal), Writing – original draft (equal), Writing – review & editing (equal)

Lorenzo Pattelli 0000-0001-5040-5282
Conceptualization (equal), Data curation (equal), Formal analysis (equal), Investigation (equal), Methodology (equal), Software (equal), Supervision (equal), Validation (equal), Visualization (equal), Writing – original draft (equal), Writing – review & editing (equal)

Alwin Kienle 0000-0001-7220-1416
Conceptualization (equal), Formal analysis (equal), Investigation (equal), Methodology (equal), Validation (equal), Visualization (equal), Writing – review & editing (equal)

Federico Tommasi 0000-0002-3178-2514
Conceptualization (equal), Formal analysis (equal), Investigation (equal), Methodology (equal), Validation (equal), Visualization (equal), Writing – review & editing (equal)

Fabrizio Martelli 0000-0001-6408-8679
Conceptualization (equal), Data curation (equal), Formal analysis (equal), Funding acquisition (equal), Investigation (equal), Methodology (equal), Software (equal), Supervision (equal), Validation (equal), Visualization (equal), Writing – original draft (equal), Writing – review & editing (equal)

Appendix. Evaluation of $\lim_{s\to 0}(s/c)(\Sigma^{-1}M)^2$

This appendix provides the details underlying the limit used in (23). We first recall why the effects of absorption can be treated independently of the long-time analysis. According to the Laplace-transform convention,

$$\mathcal{L}\{f(t)\}(s) = \hat{f}(s) := \int_0^\infty f(t)\,\mathrm{e}^{-st}\,\mathrm{d}t, \tag{37}$$

consequently,

$$\mathcal{L}\left\{\mathrm{e}^{-\mu t} f(t)\right\}(s) = \hat{f}(s+\mu)\,. \tag{38}$$

In the anisotropic P_N representation used in section 2.2, absorption changes the diagonal entries from

$$\sigma_\ell = \mu_\mathrm{s}(1-f_\ell) + \frac{s}{c}$$

to

$$\sigma_\ell = \mu_\mathrm{s}(1-f_\ell) + \frac{s+\mu_\mathrm{a}c}{c}.$$

Thus, absorption corresponds to the uniform Laplace shift $s \mapsto s+\mu_\mathrm{a}c$. It may therefore be omitted while evaluating the scattering-controlled long-time limit and subsequently restored through multiplication by $\mathrm{e}^{-\mu_\mathrm{a}ct}$.

We now evaluate the matrix limit by setting

$$A := \Sigma^{-1}M, \qquad \Sigma^{-1} = \mathrm{diag}(1/\sigma_0, \ldots, 1/\sigma_N),$$

and after removing absorption, we obtain

$$\sigma_0 = \frac{s}{c}, \qquad \sigma_\ell = \mu_\mathrm{s}(1-f_\ell) + \frac{s}{c} \quad (\ell \geqslant 1)\,.$$

The nonzero entries of A are

$$A_{k\ell} = \frac{1}{\sigma_k}\left[\frac{k}{\sqrt{4k^2-1}}\delta_{k,\ell+1} + \frac{k+1}{\sqrt{4(k+1)^2-1}}\delta_{k,\ell-1}\right], \tag{39}$$

for $k,\ell=0,\ldots,N$, with entries outside the truncated matrix omitted. Squaring this tri-diagonal matrix gives

$$\left(A^2\right)_{k\ell}=\begin{cases}\frac{1}{\sigma_k\sigma_{k+1}}\frac{k+1}{\sqrt{4(k+1)^2-1}}\frac{k+2}{\sqrt{4(k+2)^2-1}}, & \ell=k+2,\\ \frac{1}{\sigma_{k-1}\sigma_k}\frac{k^2}{4k^2-1}+\frac{1}{\sigma_k\sigma_{k+1}}\frac{(k+1)^2}{4(k+1)^2-1}, & \ell=k,\\ \frac{1}{\sigma_{k-1}\sigma_k}\frac{k-1}{\sqrt{4(k-1)^2-1}}\frac{k}{\sqrt{4k^2-1}}, & \ell=k-2,\\ 0, & \text{otherwise.}\end{cases} \tag{40}$$

The prefactor s/c in (23) selects only terms containing one factor $\sigma_0=s/c$ in the denominator. All entries whose denominators do not contain σ_0 vanish, since

$$\lim_{s\to0}\frac{s/c}{\sigma_j\sigma_m}=0\qquad\text{whenever } j,m\geqslant1. \tag{41}$$

Consequently, only the entries involving $\sigma_0\sigma_1$ can survive. From (40), these are

$$\left(A^2\right)_{00}=\frac{1}{3\sigma_0\sigma_1},\qquad \left(A^2\right)_{02}=\frac{2}{3\sqrt{5}}\frac{1}{\sigma_0\sigma_1},\qquad \left(A^2\right)_{11}=\frac{1}{3\sigma_0\sigma_1}+\frac{4}{15\sigma_1\sigma_2}. \tag{42}$$

The second term in $(A^2)_{11}$ vanishes by (41). Since $\sigma_1\to\mu_s(1-f_1)=\mu_s'$ as $s\to0$, we obtain

$$\lim_{s\to0}\frac{s}{c}\left(A^2\right)_{00}=\frac{1}{3\mu_s'}\equiv D,\qquad \lim_{s\to0}\frac{s}{c}\left(A^2\right)_{02}=\frac{2}{\sqrt{5}}D,\qquad \lim_{s\to0}\frac{s}{c}\left(A^2\right)_{11}=D. \tag{43}$$

All remaining entries vanish. Hence, for any truncation order sufficiently large to include the displayed entries, with the obvious truncation for lower orders,

$$\lim_{s\to0}\frac{s}{c}\left(\Sigma^{-1}M\right)^2=\begin{bmatrix}D & 0 & \frac{2}{\sqrt{5}}D & 0 & \cdots\\ 0 & D & 0 & 0 & \cdots\\ 0 & 0 & 0 & 0 & \cdots\\ \vdots & \vdots & \vdots & \vdots & \ddots\end{bmatrix},\qquad D=\frac{1}{3\mu_s'}. \tag{44}$$

This is the matrix limit used in (23). It shows that the leading long-time moment structure is independent of the chosen P_N truncation order, since the surviving block depends only on the first two angular moments.

References

[1] Case K and Zweifel P 1967 *Linear Transport Theory Addison-Wesley Series in Nuclear Engineering* (Addison-Wesley Publishing Company)
[2] Furutsu K and Yamada Y 1994 *Phys. Rev. E* **50** 3634
[3] Polishchuk A Y, Gutman S, Lax M and Alfano R 1997 *J. Opt. Soc. Am. A* **14** 230–4
[4] Bassani M, Martelli F, Zaccanti G and Contini D 1997 *Opt. Lett.* **22** 853–5
[5] Nakai T, Nishimura G, Yamamoto K and Tamura M 1997 *Phys. Med. Biol.* **42** 2541
[6] Cai W, Xu M, Lax M and Alfano R 2002 *Opt. Lett.* **27** 731–3
[7] Contini D, Martelli F and Zaccanti G 1997 *Appl. Opt.* **36** 4587–99
[8] Martelli F, Binzoni T, Del Bianco S, Liemert A and Kienle A 2022 *Light Propagation Through Biological Tissue and Other Diffusive Media: Theory, Solutions and Validation* 2nd edn (SPIE Press)
[9] Pierrat R, Greffet J J and Carminati R 2006 *J. Opt. Soc. Am. A* **23** 1106–10
[10] Re R, Spinelli L, Martelli F, Di Sieno L, Bargigia I, Amendola C, Maffeis G and Torricelli A 2025 *Riv. Nuovo Cimento* **48** 157–239
[11] Wojtkiewicz S, Durduran T and Dehghani H 2017 *Biomed. Opt. Express* **9** 41–54
[12] Wheelock M D, Culver J P and Eggebrecht A T 2019 *Rev. Sci. Instrum.* **90** 051101
[13] Helton M, Mycek M A and Vishwanath K 2022 *Biomed. Opt. Express* **13** 1595–608
[14] Damagatla V, Karremans S, Bossi A, Martinenghi E, Manohar S, Taroni P, Cubeddu R, Pifferi A and Bargigia I 2026 *Sci. Data* **13** 261
[15] Lindell D B and Wetzstein G 2020 *Nat. Commun.* **11** 4517
[16] Du D, Jin X, Deng R, Kang J, Cao H, Fan Y, Li Z, Wang H, Ji X and Song J 2022 *Nat. Commun.* **13** 3234
[17] Deng R, Jin X, Du D and Li Z 2023 *Opt. Express* **31** 23662–77
[18] Jin X, Du D, Jin J and Fan Y 2024 *Opt. Express* **32** 37247–59
[19] Radford J and Faccio D 2023 *Phys. Rev. Res.* **5** L022008
[20] Cheng X, Chen H, Sie E J, Marsili F and Boas D A 2022 *J. Biomed. Opt.* **27** 083009
[21] Chen H, Montanari C, Shanker R, Marcinkevicius S, Berglund L A and Sychugov I 2022 *Adv. Opt. Mater.* **10** 2102732
[22] Stefanov A, Tijkorte P, Hannink G, Roth L and Frenz M 2023 *Opt. Lett.* **48** 6396–9
[23] Schirmacher W and Ruocco G 2023 *Condens. Matter Phys.* **26** 33604

[24] Aronson R and Corngold N 1999 *J. Opt. Soc. Am. A* **16** 1066–71
[25] Durian D and Rudnick J 1997 *J. Opt. Soc. Am. A* **14** 235–45
[26] Durian D 1998 *Opt. Lett.* **23** 1502–4
[27] Ishimaru A 1978 *Wave Propagation and Scattering in Random Media* (Academic)
[28] Graaff R and Ten Bosch J 2000 *Opt. Lett.* **25** 43–45
[29] Durduran T, Yodh A, Chance B and Boas D 1997 *J. Opt. Soc. Am. A* **14** 3358–65
[30] Ripoll J, Yessayan D, Zacharakis G and Ntziachristos V 2005 *J. Opt. Soc. Am. A* **22** 546–51
[31] Yamada Y, Suzuki H and Yamashita Y 2019 *Appl. Sci.* **9** 1127
[32] Graaff R and Rinzema K 2001 *Phys. Med. Biol.* **46** 3043
[33] Heizler S I, Krief M and Assaf M 2024 *Phys. Rev. Res.* **6** L012023
[34] Liemert A and Kienle A 2011 *Phys. Rev. E* **83** 036605
[35] Liemert A and Kienle A 2012 *Phys. Rev. E* **86** 036603
[36] Liemert A and Kienle A 2012 *Biomed. Opt. Express* **3** 543–51
[37] Liemert A, Reitzle D and Kienle A 2017 *Sci. Rep.* **7** 3819
[38] Abramowitz M and Stegun I A 1964 *Handbook of Mathematical Functions with Formulas, Graphs and Mathematical tables* (*Applied Mathematics Series no 55*) (National Bureau of Standards)
[39] Liemert A 2011 Analytische Lösungen der Strahlungstransfergleichung und ihrer Approximationen *PhD Thesis Universität Ulm*
[40] Liemert A and Kienle A 2011 *Phys. Rev. A* **83** 015804
[41] Holte G 1948 *Arkiv Mat. Astron. Fysik* **35A** 1–9
[42] Graaff R, Aarnoudse J G, de Mul F F and Jentink H W 1993 *Opt. Eng., Bellingham* **32** 244–52
[43] Wang L V and Wu H 2012 *Biomedical Optics: Principles and Imaging* (Wiley)
[44] Ripoll Lorenzo J 2012 *Principles of Diffuse Light Propagation: Light Propagation in Tissues With Applications in Biology and Medicine* (World Scientific Publishing)
[45] Tricoli U, Macdonald C M, Silva A D and Markel V A 2018 *J. Opt. Soc. Am. A* **35** 356–69
[46] Kim A D and Ishimaru A 1998 *Appl. Opt.* **37** 5313–9
[47] Elaloufi R, Carminati R and Greffet J J 2003 *J. Opt. Soc. Am. A* **20** 678–85
[48] Davis A B, Polonsky I N and Marshak A 2009 space-time green functions for diffusive radiation transport *Appl. to Active and Passive Cloud Probing Light Scattering Reviews 4: Single Light Scattering and Radiative Transfer* ed A A Kokhanovsky (Springer) pp 169–292
[49] Machida M, Panasyuk G Y, Schotland J C and Markel V A 2009 *J. Opt. Soc. Am. A* **26** 1291–300
[50] Capart A, Ikegaya S, Okada E, Machida M and Hoshi Y 2021 *J. Phys. Commun.* **5** 025012
[51] Grosjean C 1956 *Il Nuovo Cimento (1955-1965)* **3** 1262–75
[52] Grosjean C 1962 A new approximate one-velocity theory for treating both isotropic and anisotropic multiple scattering problems. Part I. Infinite homogeneous scattering media *Technical Report (Universiteit,* Ghent)
[53] d'Eon E 2013 *Transp. Theory Stat. Phys.* **42** 237–97
[54] Kienle A and Patterson M S 1997 *J. Opt. Soc. Am. A* **14** 246–524
[55] Pattelli L n.d. RTEsolutions *GitHub* (available at: https://github.com/lpattelli/RTEsolutions)